STRUCTURE AND DYNAMICS OF Zr^{4+} IN AQUEOUS SOLUTION: AN AB INITIO QM/MM MOLECULAR DYNAMICS STUDY

Suwardi[1,2], Harno Dwi Pranowo[2] and Ria Armunanto[2,*]

[1]*Department of Chemistry Education, Faculty of Mathematics and Natural Sciences, Yogyakarta State University, Jl. Colombo 1, Yogyakarta, Indonesia*

[2]*Austrian-Indonesian Centre for Computational Chemistry, Department of Chemistry, Faculty of Mathematics and Natural Sciences, Universitas Gadjah Mada, Sekip Utara, Yogyakarta 55281 Indonesia*

Received October 6, 2014; Accepted March 2, 2015

ABSTRACT

A QM/MM molecular dynamics (MD) simulation has been carried out using three-body corrected pair potential to investigate the structural and dynamical properties of Zr^{4+} in dilute aqueous solution. Structural data in the form of radial distribution function, coordination number distribution, and angular distribution function were obtained. The results indicate eight water molecules coordinate to zirconium ion and have two angles of O-Zr^{4+}-O, i.e. 72.0° and 140.0° with a Zr^{4+}-O distance of 2.34 Å. According to these results, the hydration structure of Zr^{4+} ion in water was more or less well-defined square antiprismatic geometry. The dynamical properties have been characterized by the ligand's mean residence time (MRT) and Zr^{4+}-O stretching frequencies. The inclusion of the three-body correction was important for the description of the hydrated Zr^{4+} ion, and the results indicated in good agreement with experimental values.

Keywords: *hydration; ions in solution; molecular dynamics; QM/MM; Zr^{4+}*

ABSTRAK

Simulasi Dinamika Molekuler (DM) MK/MM menggunakan potensial pasangan terkoreksi potensial tiga badan telah digunakan untuk menyelidiki sifat-sifat struktur dan dinamika Zr^{4+} dalam larutan berair encer. Data struktural dalam bentuk fungsi distribusi radial, distribusi bilangan koordinasi, dan fungsi distribusi sudut telah berhasil dianalisis. Hasil analisis menunjukkan delapan molekul air terkoordinasi pada ion zirkonium dengan dua sudut O-Zr^{4+}-O, yaitu 72,0° dan 140,0° dan jarak Zr^{4+}-O 2,34 Å. Sesuai data ini, maka geometri struktur hidrasi ion Zr^{4+} dalam air adalah bujursangkar antiprismatik. Sifat dinamika dikarakterisasi melalui waktu tinggal rata-rata ligan dan frekuensi ulur Zr^{4+}-O. Penambahan koreksi tiga badan penting dalam menggambarkan hidrasi ion Zr^{4+} dan hasilnya sesuai dengan harga eksperimental.

Kata Kunci: *hidrasi; ion dalam larutan; dinamika molekuler; MK/MM; Zr^{4+}*

INTRODUCTION

Structure and dynamics hydrated Zr^{4+} have been a challenging subject for experimentalist and theoretician. The structure of the hydrated Zr^{4+} ions has been determined in concentrated aqueous perchloric acid by means of EXAFS, with the ion being eight-coordinated, most probably in square antiprismatic fashion, with mean Zr^{4+}–O bond distances of 2.187 Å [1].

The Zr has a low neutron capture cross-section and a high resistance to corrosion and as an essential commodity for the nuclear industry. Present interest in the solution chemistry of Zr arises from several perspectives including the problem of radioactive waste management [2].

It is well known, zirconium and hafnium have very similar chemical properties. Zirconium metal should contain less than 100 ppm hafnium for use in nuclear reactors. For this reason, it is necessary to separate the hafnium from zirconium, although complicated and expensive separation methods are required to remove the hafnium. At the present time, solvent extraction processes are employed on a commercial scale to separate hafnium from zirconium [3]. In solvent extraction a mixtures of immiscible solvents is used. One of those solvents is water at common. However, the zirconium ion in aqueous solution was solvated forming several layers of solvent molecules corresponding to solvation shells. The reactivity of Zr^{4+} ion is determined by the structure and dynamics of its solvation. Therefore, a detailed knowledge of the

* Corresponding author. Tel/Fax : +62-274-545188
Email address : ria.armunanto@ugm.ac.id

structural and dynamical properties of this hydrate is highly desirable in the development of solvent extraction methods especially for separation of zirconium.

The structure of $ZrOCl_2 \cdot 8H_2O$ was analyzed by the EXAFS method. The Zr^{4+}–O distance in this crystal is 2.22 ± 0.02 Å [4]. In general experiments investigations were used to determine the structure and dynamics of metal ions in solution by a variety of spectroscopic techniques such as nuclear magnetic resonance (NMR), extended X-ray absorption fine structure spectroscopy (EXAFS), Mössbauer, infrared (IR), and Raman spectroscopy, and scattering techniques such as X-ray, electron and neutron diffraction, and by theoretical methods, mostly simulations of the Monte Carlo (MC), quantum mechanics/molecular mechanics molecular dynamics (QM/MM MD) and quantum mechanics charge field (QMCF) [5-6].

Besides experimental investigations, computer simulations especially using QMCF-MD methods was applied to characterize the hydration of Zr^{4+}, U^{4+}, Np^{4+}, Ce^{4+}, and Hf^{4+} ions [7-9]. However, the methods of classical and QM/MM MD was used to evaluate structure of trivalent ions such as Cr^{3+}, Co^{3+}, Ti^{3+}, La^{3+}, Bi^{3+}, and Al^{3+} successfully whereas for tetravalent ions (M^{4+}) were unknown so far [10-13]. Hence, Zr^{4+} as one of tetravalent ions was interesting to investigate by the QM/MM MD method. In this study, the Zr^{4+} in aqueous solution was reinvestigated using QM/MM MD simulation based on three-body corrected pair potential to achieve a reliable description of the structure and dynamics of the Zr^{4+} hydrate.

METHODS

Selection of Basis Sets

The basis sets of DZP for H_2O and the modified LANL2DZ ECP for Zr^{4+} ion were selected in calculating energy of water-Zr^{4+} ion interactions. In particular, the basis sets of LANL2DZ ECP was modified because the charge transfer effects due to larger Zr^{4+}-water distances, and deviating from Lennard-Jones (12-6) curve profile as shown in Fig. 1. The modification of LANL2DZ ECP was performed by removing some basis functions with exponents below 0.5 so that this charge transfer effects were not occurred. That modification is reasonable in physical term as Zr^{4+} ion radius (0.7 Å) is much smaller than Zr atom radius (1.54 Å) for which the more diffuse basis functions have been adopted. The global minimum energies obtained by the original and the modified basis sets are -200.00 and -141.22 kcal/mol at the identical $r_{Zr^{4+}\text{-}O}$ of 2.2 Å for Zr^{4+}. Because the calculations were carried out to construct pair potential functions for classical MD simulations, the observed increase in energy could be tolerated, as the absolute energy values do not play such an important role for the evaluation of structural properties [14].

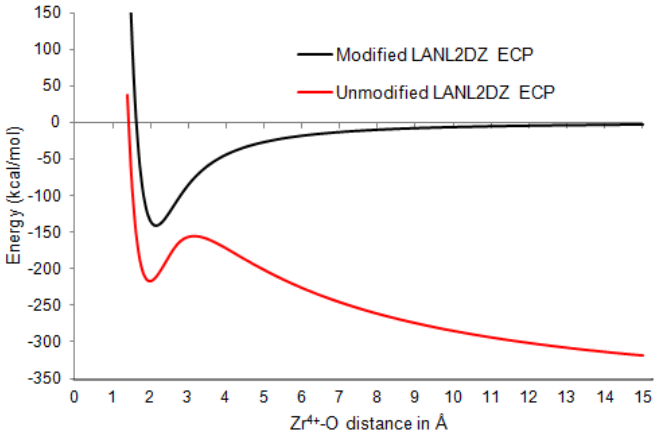

Fig 1. Energy curves for Zr^{4+}–water interactions are obtained from ab initio calculations with unmodified and modified LANL2DZ ECP basis sets

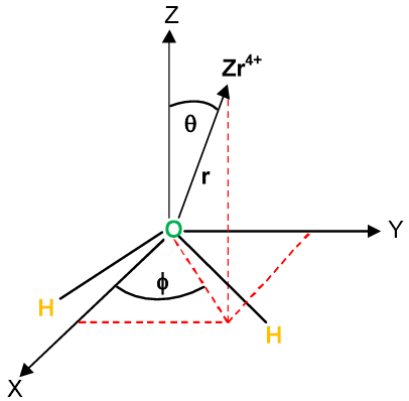

Fig 2. Definition of geometric variables for Zr^{4+}-H_2O configuration

Construction of Ion-Water Pair Potential

To construct the Zr^{4+}-H_2O pair potential, we must adjusted some geometrical parameters like distances and angles. The Zr^{4+} ion was placed at numerous positions around the water molecule by varying geometrical parameters $0° \le \theta \le 180°$ and $0° \le \phi \le 90°$; for each configuration, the Zr^{4+}-O internuclear distance r was varied from 1.4 to 15.0 Å (Fig. 2). The internal geometric parameters of water were held fixed at the experimental values, i.e., r_{OH} = 0.960 Å and ∠HOH = 104.47° [15]. The quantum mechanics calculations were performed at the RHF level using the TURBOMOLE program [16]. The interaction energies, $\Delta E_{2bd,}$ between zirconium ion and water were calculated species Zr^{4+} and H_2O are denoted by $E_{Zr(H_2O)^{4+}}$, $E_{Zr^{4+}}$,

Table 1. The optimized parameters of the analytical 2-body potential function of Zr^{4+} -water interactions in $Å^m$ kcal/mol (m is exponent according to Eq. (3)) and the analytical 3-body potential function of water-Zr^{4+}-water interactions

2-body				
	A_O	B_O	C_O	D_O
Zr^{4+}-O	-10227.48	409574.39	-1826459.83	1570267.42
	A_H	B_H	C_H	D_H
Zr^{4+}-H	-540.73	2657.28	-2086.54	274.31
3-body				
	F(kcal/mol $Å^{-4}$)		G($Å^{-1}$)	H($Å^{-1}$)
H_2O-Zr^{4+}-H_2O	0.1699019		0.4868692	-0.3429535

and E_{H_2O}, respectively [17-18].

$$\Delta E_{2bd} = E_{Zr(H_2O)^{4+}} - E_{Zr^{4+}} - E_{H_2O} \quad (1)$$

More than 8000 water-ion configurations were used in the construction of the pair potential using a modified LANL2DZ ECP basis sets for Zr^{4+} and Dunning DZP basis sets for oxygen and hydrogen. The 2-body energies were fitted to an analytical form,

$$\Delta E_{Fit}^{2bd} = \sum_{i=1}^{n} \frac{q_M q_i}{r_{Mi}} + \frac{A_i}{r_{Mi}^a} + \frac{B_i}{r_{Mi}^b} + \frac{C_i}{r_{Mi}^c} + \frac{D_i}{r_{Mi}^d} \quad (2)$$

where M denotes metal ions, i solvent atoms, n the number of atoms in solvent molecule, A, B, C, and D are optimized parameters and q represents the atomic charge. The a, b, c and d are exponents (m) taking values in a range from 4–12. For Zr^{4+}-H_2O system, the equation (2) becomes,

$$\Delta E_{Fit}^{2bd} = \frac{q_O q_{Zr^{4+}}}{r_{Zr^{4+}-O}} + \frac{A_O}{r_{Zr^{4+}-O}^5} + \frac{B_O}{r_{Zr^{4+}-O}^9} + \frac{C_O}{r_{Zr^{4+}-O}^{11}} + \frac{D_O}{r_{Zr^{4+}-O}^{12}} + \sum_{i=1}^{2} \left(\frac{q_H q_{Zr^{4+}}}{r_{Zr^{4+}-H_i}} + \frac{A_H}{r_{Zr^{4+}-H_i}^4} + \frac{B_H}{r_{Zr^{4+}-H_i}^5} + \frac{C_H}{r_{Zr^{4+}-H_i}^6} + \frac{D_H}{r_{Zr^{4+}-H_i}^{12}} \right) \quad (3)$$

The charges were set to 4.0 for Zr^{4+} and -0.6598 and 0.3299 for O and H, respectively, corresponding to the BJH-CF2 water model. The final parameters for 2-body potential function are listed in Table 1.

Construction of Analytical 3-Body Function

Construction of 3-body potential as a correction of 2-body potential based on interaction energies of three species, H_2O-Zr^{4+}-H_2O. To construct it, more than 17,000 interaction points of H_2O-Zr^{4+}-H_2O was calculated using the TURBOMOLE program. The obtained data were fitted to an analytical form by Levenberg-Marquardt algorithm.

$$E_{3bd} = Fe^{-Gr_{12}} e^{-Gr_{13}} e^{-Hr_{23}} (r_{cut} - r_{12})^2 (r_{cut} - r_{13})^2 \quad (4)$$

the ion-oxygen distances for water molecules are denoted by r_{12} and r_{13}, respectively whereas r_{23} is the oxygen-oxygen distances between two water molecules. The cutoff radius r_{cut} is set to 6.0 Å after which 3-body effects can be ignored. The root mean square deviation (rmsd) of the fitted function was 0.8189284 kcal/mol. The final parameters F, G, H are listed in Table 1.

Simulation Protocol

The simulations were carried out in the NVT canonical ensemble, consisting of one Zr^{4+} ion and 499 water molecules in a periodic box of 24.77 at 298.16 K, which is maintained through the Berendsen algorithm. The density of system is considered to be equal to the density of pure water is 0.99702 g cm^{-3}. A cutoff of 12 Å was set except for O-H and H-H non-Coulombic interaction where it was set to 5 and 3 Å. The reaction field method was used to account for long-range electrostatic interactions. For the water-water interactions BJH-CF2 water model containing intramolecular term, has been used. In accordance with this water model, the time step of the simulation was set to 0.2 fs, which allows for explicit movement of hydrogens [19-20].

QM/MM-MD Simulation

The classical MD simulations were performed for 204 ps by two steps. The first step, simulation was run using pair potential function during 102 ps, starting from a random configuration. After which simulation continued with pair plus 3-body potentials for 102 ps. Subsequently, the QM/MM simulation was carried out for more 50 ps. The quantum mechanical treatments around the metal ion had a radius of 3.8 Å and water molecules were permitted to leave and enter from and to this region dynamically. The size of this region includes the full first hydration shell at any step of the simulation. A smoothing function was given in the transition region between QM and MM forces. The forces of system, F_{system}, is defined as:

$$F_{System} = F_{MM} + S(F_{QM} - F_{QM/MM}) \quad (5)$$

where F_{system} is the total force of system, F_{MM} is the MM

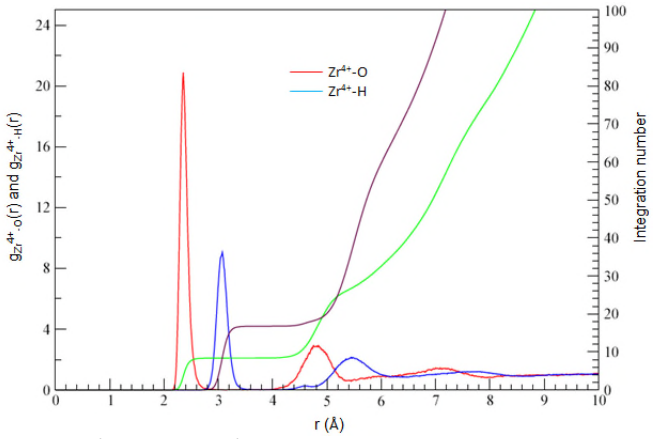

Fig 3. Zr^{4+}-O and Zr^{4+}-H radial distribution functions and their running integration numbers for Zr^{4+} in water

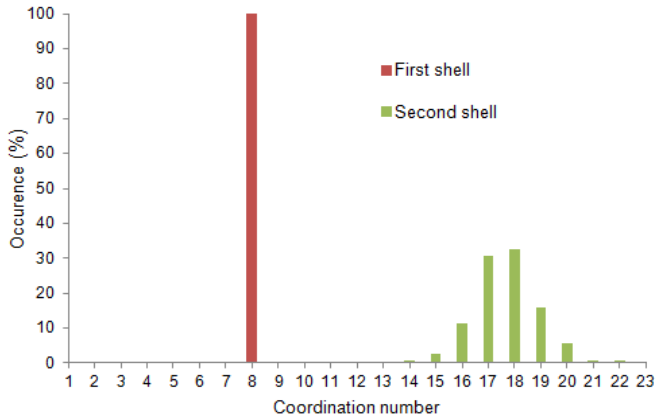

Fig 4. Coordination number distributions (CND) of the first and second hydration shell of Zr^{4+} in water obtained from a QM/MM MD simulation until 30 ps

Table 2. Comparison of hydration parameters obtained from various methods for Zr^{4+} in water

Samples	$r^{(1)}_{Zr^{4+}\text{-}O}$ (first shell)	n_1	n_2	Methods	References
1 Zr^{4+} in 499 H_2O	2.25	10	~23	2bd-Classical MD	This work
1 Zr^{4+} in 499 H_2O	2.38	8	~17	2bd+3bd-Classical MD	This work
1 Zr^{4+} in 499 H_2O	2.34	8	17.2	QM/MM MD	This work
$[Zr_4(OH)_8(OH_2)_{16}]Cl_8$(s)	2.131	-	-	XRD	[1]
$[Zr_4(OH)_8(OH_2)_{16}](ClO_4)_8$(s)	2.140	-	-	EXAFS	[1]
$Zr_4(OH)_8{}^{4+}$(aq)	2.154	-	-	EXAFS	[1]
$Zr(OH_2)_8{}^{4+}$(aq)	2.187	8	-	EXAFS	[1]
$ZrOCl_2{\cdot}8H_2O$ (s)	2.22 ± 0.02	8 ± 1	-	EXAFS	[4]
$ZrOCl_2{\cdot}8H_2O$ 0.1 M aqueous solution	2.22 ± 0.01	7.9 ± 0.8	-	EXAFS	[4]
Zr-exchanged beidellite	2.21 ± 0.01	8 ± 0.3	-	EXAFS	[4]
pillared beidel-lite (PB)	2.16 ± 0.02	6.1 ± 1.4	-	EXAFS	[4]
1 Zr^{4+} in 1000 H_2O	2.25	8	17.8	QMCF	[5]

$r^{(1)}$ is the distance in Å for the first maxima of RDF, n_1 and n_2 are the average coordination number of the first and second shell, respectively.

force of the system, F_{QM} is the QM force in the QM region and $F_{QM/MM}$ is the MM force in the QM region. The S denotes the smoothing function. Free migration of water ligand between the QM and MM region is enabled in this approach.

$$S(r)=\begin{cases}0 & \text{for } r \le r_1,\\ \dfrac{(r_0^2-r^2)^2(r_0^2+2r^2-3r_1^2)}{(r_0^2-r_1^2)^3} & \text{for } r_1<r\le r_0,\\ 1 & \text{for } r>r_0.\end{cases} \quad (6)$$

where r_1 and r_0 are the ion-water distances indicating the start and end of the shell, where smoothing applies [21-22].

RESULT AND DISCUSSION

The Zr^{4+}-O and Zr^{4+}-H radial distribution functions for QM/MM molecular dynamics simulations are shown in Fig. 3. The RDF of Zr^{4+}-O reveals well-defined structures for the first and the second hydration shell. The first shell peaks at 2.34 Å and separated from the second shell by a minimum and reaches the x- axis. This indicates ligand exchange have been not taken place along the simulation trajectory. The second shell peak of the Zr^{4+}–H RDF is overlapping with the respective peak of the Zr^{4+}–O RDF within a long range and hence, the flexibility of the second shell is very high. The third shell is almost indistinguishable from the bulk. A maximum peak is located at 4.755 Å with a broad peak observed between 4.0 and 5.4 Å corresponds to a second hydration shell containing in average of 17.2 water molecules. The Zr^{4+}-O distance of 2.34 Å is in good agreement with EXAFS investigation, namely 2.22 ± 0.02 Å [4].

The slightly larger Zr^{4+}-O bond length obtained from these simulations because of ignoring of electron correlation in the ab initio calculation although a relativistically corrected ECP was applied in the QM/MM simulations. The hydration parameters are compared with other simulations and experimental methods in Table 2. Interestingly, the bond length of the 2-bd-classical MD simulations is in good agreement with experimental and QMCF results, because the used pair potentials assume the ionic charge to be fixed,

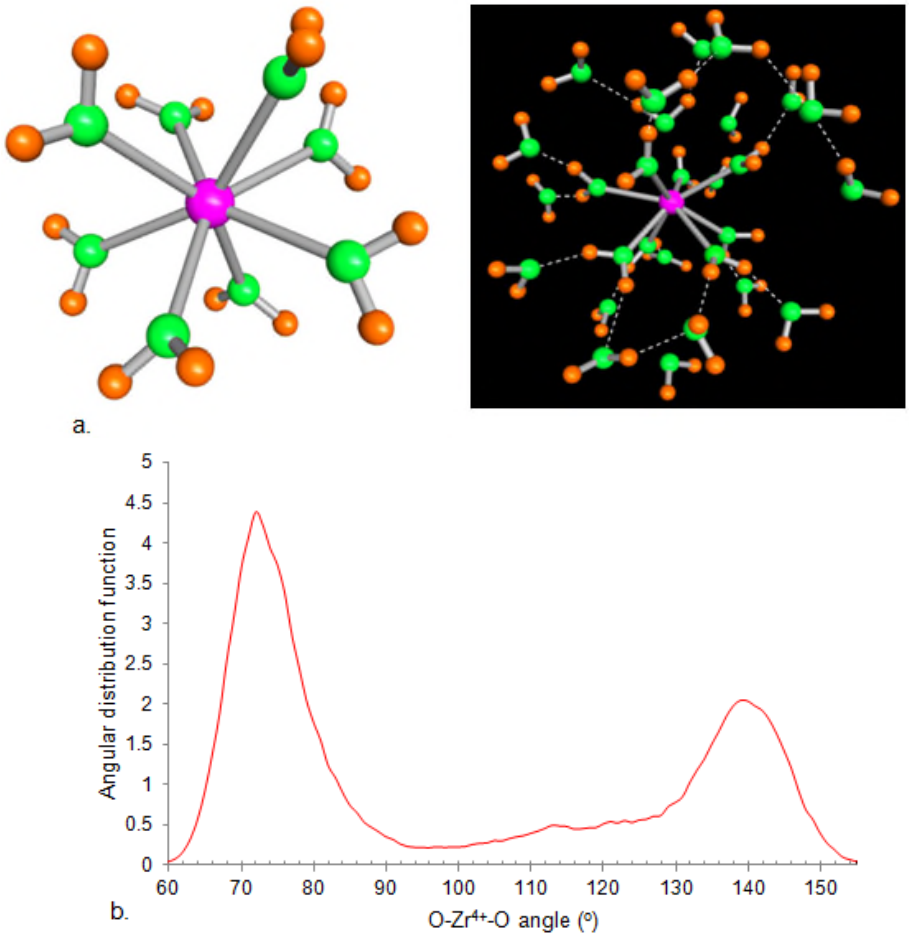

Fig 5. a. Square antiprism structure of the first hydration shell and a number of water molecules forming hydrogen bond in the second hydration shell of Zr^{4+} in water (Snapshot taken by tmolex); b. Distribution of the bond angles H_2O-Zr^{4+}-H_2O for QM/MM-MD simulations

whereas a quantum mechanical treatment accounts for all polarization and charge transfer effects and thus also the charge fluctuations on the central ion. The influence of polarization in classical simulations has been investigated by Meier et al., who indeed reported an increased ion–oxygen bond length, but no change in the coordination number [23].

The distributions of the coordination numbers in the first and the second hydration shells are evaluated, as depicted in Fig. 4. The obtained eight-coordinated complex in the first hydration shell (100% occurrence) is in agreement with EXAFS and QMCF data. This indicates the rigidity of first hydration shell structure. The coordination number for the second solvation shell range 14-20 with average of 17.2, implying that every first shell water molecule interacts with about 2.15 water molecules in the second shell.

The hydration structure may be indicated from angular distribution functions (ADF). Fig. 5 shows distribution of oxygen-zirconium-oxygen angle within the first hydration shell and snapshot a number of water molecules. The ADF peaks at 72 and 140° between the two maxima a valley ranging from 90 to 128° was observed. Two sharp peaks clearly separated from each other towards a defined structure with quite rigidity within the first shell. The square antiprism seems to match best to the structure of first hydration shell.

The orientation of water molecules in the first and second hydration shell can be discussed on the basis of two angle parameters i.e. theta and tilt angle. The theta is the angle between the Zr^{4+}-O vector and the resulting vector obtained from the sum of the O-H bonds whereas tilt is defined by the Zr^{4+}-O vector and the plane spanned by the water molecule. The theta and tilt angle distributions within the first and second hydration shell are depicted in Fig. 6. The theta angle distribution shows the highest peak at 173°, the smallest angle recorded has a value of 150° in the first shell. This narrow peak shows the low angular flexibility of ligands in the $Zr(H_2O)_8^{4+}$ complex. The weak tailing

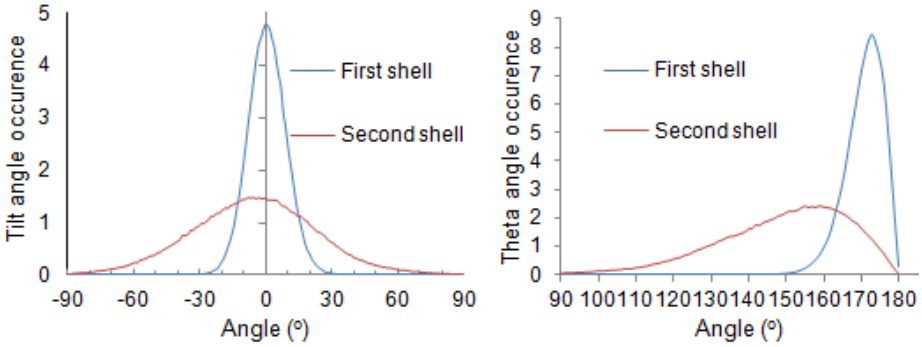

Fig 6. Tilt (Out-of-plane) angle distributions and Theta angle distributions (angle between dipole vector and Zr^{4+}–O connection vector) of first and second shell obtained by QM/MM–MD simulations

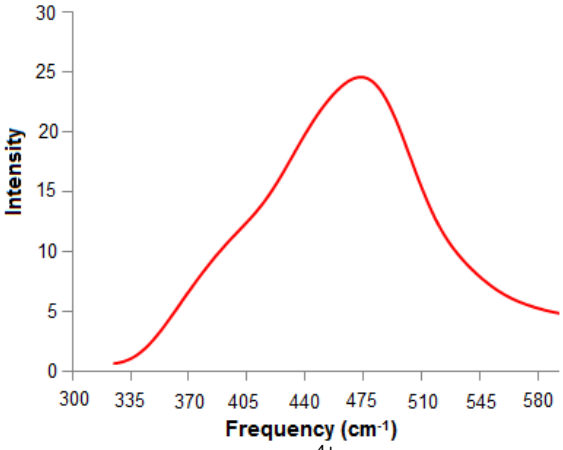

Fig 7. Power spectrum of Zr^{4+}-oxygen vibrational mode in the first hydration shell obtained by QM/MM simulations

Table 3. The parameter of H–O–H angles and O–H distances of water molecules in three phases observed in QM/MM Molecular Dynamics simulations of Zr^{4+} ion

Ion	Phase	r (O-H)/(Å)	H-O-H angle (°)
Zr^{4+}	First hydration shell	0.968	101
	Second hydration shell	0.973	101
	Bulk	0.973	101

of the θ-angle towards lower angles is related with the strong Zr^{4+}–water interaction leading to slow motion of the water molecules. Furthermore, the angles correspond to water molecules that are nearly perfectly dipole oriented. The water molecules of the second hydration shell still exhibit this feature, but with a naturally broader distribution with significant population down to about 60 and a maximum at 150. The tilt-angle distribution is very broad and the maximum at 0° (± 9° at half height) further demonstrates the high stability of the first shell ligands. As comparisons, tilt angle distribution for Zr(IV), Al(III), Ni(II) are ± 30°, ± 35°, ± 50°, respectively. The stronger polarizing ion tends to have low degree of flexibility [14].

The strong ion–ligand bonding deduced from the structural properties is reflected in the Zr^{4+}–O vibrational mode as well. The power spectra of the Zr^{4+}–O stretching motion obtained by QM/MM simulations is displayed in Fig. 7. The frequency of Zr^{4+}-O stretching mode is 476.81 cm^{-1}, the corresponding force constant 182.53 N m^{-1} while according to QMCF m ethod of 188 N m^{-1} [5]. This value indicates strong ligand bonding occurring to take place in the first hydration shell. Therefore, no frequent ligand exchange between the first and the second shell.

The values of H–O–H angles and O–H distances with the maximum intensity in the first hydration shell are about 101° and 0.968 Å, respectively as depicted in Fig. 8. Experimental gas phase values were used for the water (O–H = 0.9601 Å and H–O–H =104.47°) [9]. The Zr^{4+} ion has a small influence on the water geometry in the first shell, leading to an elongation of the O-H bond of 0.01 Å and a reduced H-O-H angle of 3.47°. The values of H–O–H angles and O–H distances observed from the simulations are summarized in Table 3.

The Zr^{4+} ion-water distance plots produced during the QM/MM simulation are depicted in Fig. 9. No water exchange between first and second hydration shell until 30 ps, illustrating the rigid of the first hydration shell and thus its stability. However, if more simulations continued, ligand migration between the first and second shell was observed. The reactivities of Zr^{4+} ions can also be known by the ligand exchange rate of water between shell hydration and bulk. The exchange rate is evaluated through the analysis of ligand residence time (MRT) of water in the second hydration shell. The MRT values were evaluated using a direct method [24-25], being the product of the average number of water molecules in the hydration shell during the duration of the simulation divided by the number of exchange events

Table 4. Mean ligand residence times (MRT) in ps, number of accounted exchange events (N_{ex}) obtained by direct method as a function of t^* and sustainability coefficient (S_{ex})

	t_{sim} /ps	t^* = 0 ps		t^* = 0.5 ps		S_{ex}	$1/S_{ex}$
		N_{ex}^0	τ	$N_{ex}^{0.5}$	τ		
Second shell[a]	50.50	6356	0.276	322	5.456	0.051	19.74
Bulk[b]	10.00	269	0.200	24	1.700	0.090	11.11

[a] As comparison, MRT = 5.5 ps using QMCF method [5]
[b] Values obtained from a QM/MM MD simulation of pure water [26]

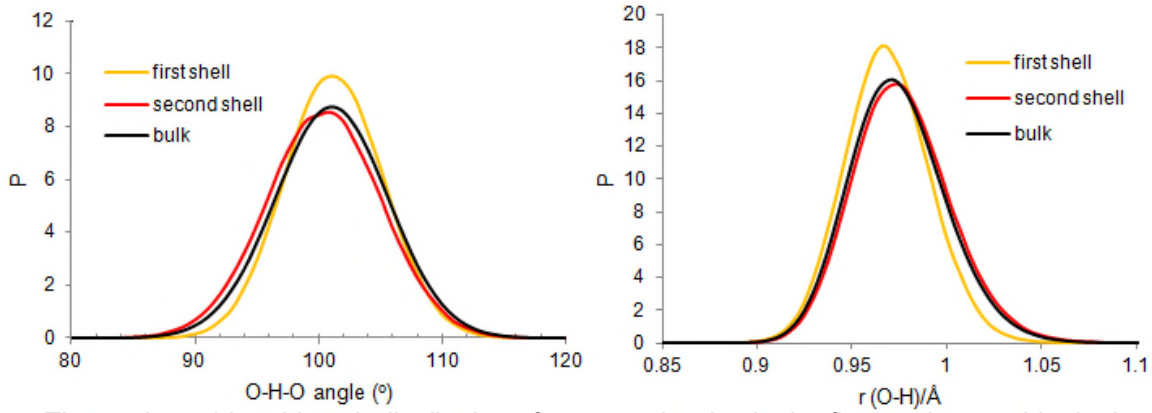

Fig 8. a. The angle and bond-length distribution of water molecules in the first, and second hydrations shell and in bulk

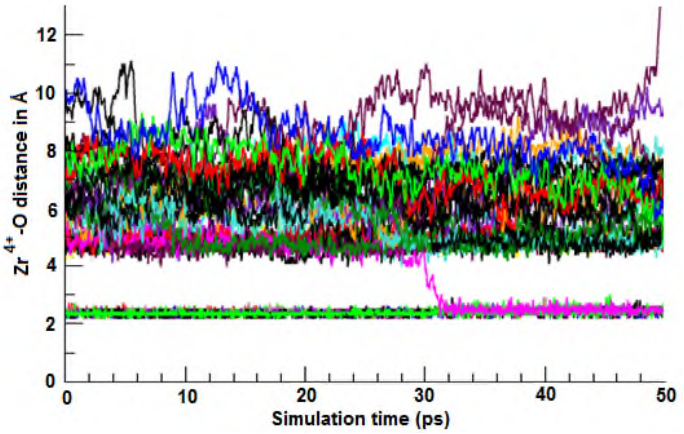

Fig 9. Variation of Zr^{4+} ion-oxygen distances during the QM/MM simulation showing no exchange processes between first and second hydration shells until 30 ps. After simulations 30 ps ligand migration was observed

Based on direct accounting and setting the time parameter t* to 0 (all movements out of shell are accounted) and 0.5 (only exchange processes leading to a longer-lasting removal of a ligand. The MRT values listed in Table 4 were obtained. Mean ligand residence times (τ) in ps and number of accounted exchange events (N_{ex}) as a function of t^* evaluated by direct method. Besides mean ligand residence times, the simulation can supply properties of ions in terms of lability of the hydration shell and sustainability of exchange processes. Sustainability measures the rates of success of exchange events in leading to longer lasting changes in the hydration structure. A sustainability coefficient (S_{ex}) can be defined as [12]:

$$S_{ex} = \frac{N_{ex}^{0.5}}{N_{ex}^{0}} \quad (7)$$

where N_{ex}^0 is the number of all transitions through a shell boundary and means the number of changes persisting after 0.5 ps. The inverse, $1/S_{ex}$, represents the average number of border-crossing attempts to produce one longer-lasting change in the hydration structure of an individual ion [14]. The MRT values in the second shell (5.456 ps) is much greater than that of water in bulk. This means that the mobility of water molecules in the second shell is smaller than in the pure solvent. The value of 0.051 was calculated for sustainability coefficient S_{ex} of Zr^{4+}, the corresponding $1/S_{ex}$ is 19.74, which means that about 20 attempts to leave or enter the second hydration shell are needed to achieve one lasting exchange process.

CONCLUSION

Based on the simulation by the QM/MM method, the hydration structure of square antiprismatic geometry of Zr^{4+} consists of eight water molecules in the first hydration shell is rigid. However, if the simulation was continued more than 30 ps, the

displacement of the water ligand of a second shell to first shell was observed. It indicated a more flexible second hydration shell. The dynamical properties of the hydration Zr^{4+} ion obtained by this method is in good agreement with QMCF method.

ACKNOWLEDGEMENT

Financial support for this work by the Dr. grant (No: 1853/E4.4/2011) from the Indonesian Government through the Directorate General of Higher Education while the software and hardware were supported by the Austrian-Indonesian Centre (AIC) for Computational Chemistry are gratefully acknowledged.

REFERENCES

1. Hagfeldt, C., Kessler, V., and Persson, I., 2004, *Dalton Trans.*, 14, 2142–2151.
2. Aja, S.U., Wood, S.A., and Williams-Jones, A.E., 1995, *Appl. Geochem*., 10, 603–620.
3. Lee, H.Y., Kim, S.G., and Oh, J.K., 2004, *Hydrometallurgy*, 73(1-2), 91–97.
4. Miehé-Brendlé, J., Khouchaf, L., Baron, J., Dred, R.L., and Tuilier, M.H., 1997, *Microporous Mater*., 11(3-4), 171–183.
5. Messner, C.B., Hofer, T.S., Randolf, B.R., and Rode, B.M., 2011, *Phys. Chem. Chem. Phys*., 13, 224–229.
6. Mohammed, A.M., 2003, *Bull. Chem. Soc. Ethiop.*, 17(2), 199–210.
7. Messner, C.B., Hofer, T.S., Randolf, B.R., and Rode, B.M., 2011, *Chem. Phys. Lett*., 501(4-6), 292–295.
8. Lutz, O.M.D., Hofer, T.S., Randolf, B.R., Weiss, A.K.H., and Rode, B.M., 2012, *Inorg. Chem.*, 51(12), 6746−6752.
9. Frick, R.J., Pribil, A.B., Hofer, T.S., Randolf, B.R., Bhattacharjee, A., and Rode, B.M., 2009, *Inorg. Chem.*, 48(9), 3993–4002.
10. Kritayakornupong, C., Yagüe, J.I., and Rode, B.M., 2002, *J. Phys. Chem. A*, 106(44), 10584–10589.
11. Hofer, T.S., Randolf, B.R., and Rode, B.M., 2006, *Chem. Phys. Lett*., 422(4-6), 492–495.
12. Durdagi, S., Hofer, T.S., Randolf, B.R., and Rode, B.M., 2005, *Chem. Phys. Lett*., 406(1-3), 20–23.
13. Armunanto, R., Schwenk, C.F., Setiaji, A.H.B., and Rode, B.M., 2003, *Chem. Phys*., 295(1), 63–70
14. Remsungnen, T., and Rode, B.M., 2004, *Chem. Phys. Lett*., 385(5-6), 491–497.
15. Hofer, T.S., Randolf, B.R., and Rode, B.M., 2006, *J. Phys. Chem. B*, 110(41), 20409–20417.
16. R. Ahlrichs, M. Br, H. Horn, M. Hser, C. Klmel, *Chem. Phys.Lett*. 162 (1989) 165.
17. Yagüe, J.I., Mohammed, A.M., Loeffler, H., and Rode, B.M., 2001, *J. Phys. Chem. A,* 105(32), 7646–7650.
18. Pranowo, H.D., Wijaya, K., Setiaji, B., and Janu, R.S., 2002, *Indones. J. Chem.*, 2(1), 1-7.
19. Armunanto, R., Schwenk, C.F., and Rode, B.M., 2003, *J. Phys. Chem. A*, 107(17), 3132–3138.
20. Tongraar, A., Liedl, K.R., and Rode, B.M., 1997, *J. Phys. Chem. A*, 101(35), 6299–6309.
21. Vchirawongkwin, V., Kritayakornupong, C., and Tongraar, A., 2011, *J. Mol. Liq.*, 163(3), 147–152.
22. Loeffler, H.H., Yagüe, J.I., and Rode, B.M., 2002, *Chem. Phys. Lett.*, 363(3-4), 367–371.
23. Hofer, T.S., Scharnagl, H., Randolf, B.R., and Rode, B.M., 2006, *Chem. Phys.*, 327(1), 31–42.
24. Kritayakornupong, C., 2007, *Chem. Phys. Lett.*, 441(4-6), 226–231.
25. Armunanto, R., Schwenk, C.F., Tran, H.T., and Rode, B.M., 2004, *J. Am. Chem. Soc.*, 126(8), 2582–2587.
26. Hofer, T.S., Tran, H.T., Schwenk, C.F., and Rode, B.M., 2004, *J. Comput. Chem*. 25(2), 211–217